Practical ultra-high-strength concrete for precast concrete applications

Ahmed Al Mohammedi, Cameron D. Murray, Canh N. Dang, and W. Micah Hale

- This paper discusses the development of ultra-high-strength concretes (UHSCs) with mechanical properties comparable to those of ultra-high-performance concrete (UHPC) and with production procedures similar to those used for high-strength concrete such that the UHSCs can be easily implemented on large-scale projects and for precast concrete applications.
- Through trial and error, three preferred mixtures were developed: UHSCs with compressive strengths of 17 and 20 ksi (117 and 138 MPa) and a UHPC with a compressive strength of 24 ksi (165 MPa).
- Laboratory tests were conducted to investigate predictions of modulus of elasticity, flexural strength, creep, and shrinkage for the developed mixtures.
- This paper demonstrates that it is practical to use UHSC in bridge girders. Using the developed UHSC mixtures and 0.7 in. (18 mm) diameter prestressing strands will produce adequate flexural strength to design 300 ft (91.4 m) long prestressed concrete I-girders whose service stresses are within safe limits.

Ultra-high-performance concrete (UHPC) has been successfully used in many highway bridges in the United States. However, the use of UHPC in the construction of prestressed concrete bridge girders is still limited, even though research has demonstrated UHPC's excellent strength and durability characteristics compared with those of conventional concrete or high-strength concrete (HSC).[1] The reasons for the limited use of UHPC are mainly the production and material costs, the need for special equipment (such as a large, high-shear-capacity mixer), and insufficient production experience with the material.[2] Because UHPC requires high proportions of silica fume, silica powder, and steel fiber, and a high dosage of water-reducing admixtures, UHPC mixtures cost several times more than conventional mixtures. Production costs are higher for UHPC because it requires longer mixing and curing operations. This paper focuses on developing economical ultra-high-strength concrete (UHSC) that can be mixed, placed, and cured with the same equipment used for conventional concrete at a precast concrete facility. This study presents a modified cross section and a flexural design for a 300 ft (91.4 m) long bridge girder using the proposed UHSC and 0.7 in. (18 mm) diameter prestressing strands.

In this paper, we use Russell and Graybeal's definition of UHPC: a cementitious-based composite material with compressive strengths greater than 21.7 ksi (150 MPa).[3] We define UHSC as concrete with compressive strengths between 15 and 21.7 ksi (103 and 150 MPa).

Most UHPC mixtures are characterized by very low water-binder ratios *w/b*—as low as 0.145—and require several days of moist and heat curing.[4,5] Using such mixtures in a large-scale project may not be practical or economical. Any adjustment to the typical mixing, placing, and curing standards in precast concrete plants would require significant equipment and procedural changes, which may be difficult to implement. Concrete made using typical precast concrete plant equipment and procedures but with compressive strengths up to 20 ksi (138 MPa) would be more practical to implement than UHPC mixtures and could provide nearly the same strength and density benefits as UHPC.

Another reason UHPC has not been widely adopted in the precast, prestressed concrete industry is that compressive strength is not the only factor to consider when optimizing the design of prestressed concrete bridge girders. Girder weight, shipping practicalities, erection considerations, and lateral stability can limit the feasible span length and cross-section dimensions of a girder even if the girder is structurally improved in terms of flexural or shear capacity. UHSC can offer comparable advantages to UHPC in terms of strength while potentially overcoming UHPC's limitations. For instance, the use of coarse aggregate in UHSC results in concrete with a higher modulus of elasticity (MOE) than that of UHPC, as we will discuss in the following sections.

It is common for today's precast concrete plants to produce HSC. Most long-span bridge girders contain concrete with compressive strengths up to 12 ksi (83 MPa).[6] Advances in concrete admixtures and the use of pozzolanic materials make it feasible to produce concrete with a compressive strength greater than 12 ksi. Therefore, practical UHSC should be widely used in more projects to take advantage of the enhanced concrete properties.[7] The use of UHSC in precast and prestressed concrete components increases stiffness and reduces long-term deformations of the concrete that cause loss of prestress. In bridge girders, UHSC increases the structural capacity and reduces the number of girders required for a given span compared with conventional precast concrete. To use the UHSC proposed in this paper for precast concrete applications, it is important to assess the applicability of the current design equations in predicting creep, shrinkage, MOE, and flexural strength for UHSC.

Previous studies on UHSC and UHPC for precast concrete applications

Because of their control of mixing and curing conditions, precast concrete plants have a high potential to successfully implement UHSC mixtures. Several studies have been conducted to provide practical UHSC for the bridge community. Achieving high compressive strength was a focus in several studies. Tadros and Morcous[2] tested several trial batches to obtain 18 ksi (124 MPa) UHPC at a lower cost than commercially available UHPC mixtures. The study proposed two mixtures to be used in precast concrete members. Both mixtures contain silica fume and Class C fly ash with a very low water-binder ratios *w/b* (**Table 1**). The compressive strengths of the two mixtures exceeded 12 ksi (83 MPa) at 24 hours, 15 ksi (103 MPa) at 28 days, and 16 ksi (110 MPa) at 56 days. All test specimens were subjected to 1 day of heat curing with oven temperatures up to 135°F (57°C) followed by moist curing until the time of testing. Because of the very low water-binder ratios *w/b* and the use of silica fume, a high-shear mortar mixer was needed to achieve adequate mixing.

Giesler et al.[4] investigated the feasibility of mixing, casting,

Table 1. Ultra-high-performance concrete mixtures for precast concrete applications

Material	Tadros and Morcous (2009)		Weldon et al. (2010)	Giesler et al. (2016)
Portland cement, lb/yd³	1120	1050	1264	1296
Silica fume, lb/yd³	240	150	158	203
Class C fly ash, lb/yd³	240	300	158	122
Sand, lb/yd³	2255	1580	1900	1812
Coarse aggregate, lb/yd³	0	672.3	0	0
High-range water-reducing admixture, lb/yd³	70	54	76.5	82.1
Steel fiber, lb/yd³	0	0	200	198
Water, lb/yd³	265	245	221.2	258
Water-binder ratio *w/b*	0.166	0.163	0.140	0.159
Compressive strength, ksi	16.51	17.51	23.43	23.0
Curing procedure	1 day of heating + 90 days of moist curing		6 days of heating	

Note: 1 lb/yd³ = 0.5933 kg/m³; 1 ksi = 6.895 MPa.

and curing UHPC in a precast concrete plant. The UHPC mixture proportions were designed to obtain a target compressive strength of 20 ksi (138 MPa) by incorporating silica fume, fly ash, steel fiber, and a high dosage of high-range water-reducing admixture (HRWRA), with a water-binder ratio *w/b* of 0.145. The UHPC was used to cast several beam specimens ranging from small prisms (6.0 × 6.0 × 36 in. [150 × 150 × 914 mm]) to 6.0 in. × 9.0 in. × 13 ft (150 mm × 230 mm × 3.7 m) prestressed beams. The study evaluated the production feasibility of UHPC in a precast concrete plant and provided recommendations such as using form vibration to ensure proper consolidation, using a high-energy mixer to minimize mixing time, and allowing a minimum of 24 hours for the concrete to achieve an initial set before steam curing.

Weldon et al.[8] investigated the benefits and the limitations of using UHSC and UHPC in prestressed concrete bridge design in New Mexico. Through a case study of two local bridges, the investigators concluded that using UHPC with compressive strengths in the range of 15 to 22.5 ksi (103 to 155 MPa) led to significant reductions in the number of girders required while also reducing or eliminating the need for mild steel shear reinforcement. Bridges built with UHPC members could also provide at least twice the service life expected from bridges using conventional precast concrete. Although the study proposed optimizing UHPC mixture proportions to obtain a compressive strength around 22 ksi (152 MPa), the curing regimen included a 7-day heat cure, which is probably unrealistic for a typical precast concrete facility.

From the studies discussed and several others available,[1,9,10] it can be concluded that using UHPC in a precast concrete plant requires casting, curing, and placing procedures that are different from those used to produce HSC. These requirements limit the use of UHPC in large-scale projects and makes producing UHPC members impractical for most precasters. Developing a UHSC mixture that can be mixed, placed, and cured in large quantities using the same procedures followed for conventional concrete would be very beneficial in terms of design and durability.[8,11] This project focused on developing practical mixtures with compressive strengths comparable to those of UHPC. Most importantly, the new mixtures can be implemented in precast concrete facilities without needing special procedures or equipment for mixing, placing, and curing.

Developing UHSC mixtures

Considering the established limitations of UHPC for precast concrete plant applications, the goal of this study was to create two mixtures that are feasible for use in bridge girder construction. The targeted compressive strengths were 17 to 20 ksi (117 to 138 MPa). A minimum spread of 25 in. (635 mm) in inverted slump flow was targeted to ensure a sufficient workability for the pumping, placing, and finishing of concrete. A 1-day accelerated curing regimen was planned, followed by moist curing until the testing age. This curing regimen can be practical to implement, and it is already widely used in precast concrete plants.

Silica fume is essential in UHPC mixtures and is one of the primary materials used to increase strength and durability.[5] The pozzolanic reaction of silica fume produces additional calcium silicate hydrates (C-S-H) that fill voids in the paste;[9] however, the cost of silica fume can be as much as seven times the cost of portland cement. In addition, the large surface area of silica fume particles results in higher water demand and increases the amount of HRWRA needed for adequate workability. Silica fume content must be carefully balanced to obtain the target compressive strength at an acceptable cost. Two types of silica fume were used through-

Densified silica fume

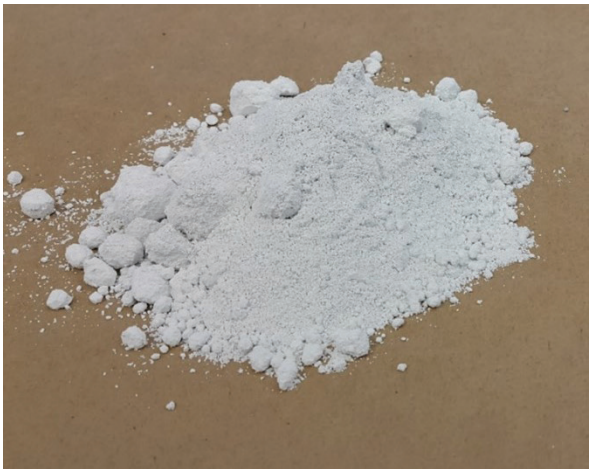

Undensified silica fume

Figure 1. Densified silica fume and undensified silica fume.

out this study (**Fig. 1**). Densified gray silica fume was used to obtain the 20 ksi (138 MPa) UHSC and the 24 ksi (165 MPa) UHPC. The undensified white silica fume was used for the 25 ksi (172 MPa) UHPC.

Class C fly ash seems to be the most economical solution to increase the ultimate strength, durability, and workability of UHPC. Class C fly ash is available in U.S. markets at about one-third the price of portland cement. Perhaps the only downside of the fly ash is that it reduces the early-age strength of the concrete, thereby limiting its widespread use in prestressed concrete girders. The UHSC mixtures developed in this study contain the maximum amount of fly ash that can be used while maintaining the targeted early-age strengths.

Steel fiber is one of the main components used in UHPC. Steel fibers increase the ductility, tensile strength, and flexural strength of precast concrete members.[12,13] However, steel fibers are the most expensive component of UHPC. The cost of steel fiber makes implementing UHPC in a large-scale project challenging unless the expense is offset by replacing some or all the mild steel shear reinforcement with steel fiber. In this study, steel fibers were added to the final mixture proportions to increase the tensile strength. In a bridge girder, the tensile stress in the bottom concrete fibers at midspan must be less than specified limits to prevent concrete cracking under the Service III limit state.[14] When determining the span length and the number of prestressing strands for a girder design, this limit governs in most cases. Using steel fibers in the concrete increases the allowable tensile stresses, which means span lengths can be increased without causing flexural cracks.

Different sizes of crushed limestone were used as a coarse aggregate. After a trial-and-error investigation of the strength and workability of several batches, it was determined that crushed limestone with a maximum size of ¼ in. (6.4 mm) had the greatest potential to produce the desired workability and strength. This aggregate also led to noticeable increases in the MOE and reductions in creep strains, as will be discussed later in this paper.

An accelerated curing regimen was used to obtain the initial material proportions that provided the highest strengths. Twenty-four hours after casting, the concrete cylinders were placed in a water tank set at 140°F (60°C) for 3 days, followed by 2 days at 194°F (90°C). After heat curing, the specimens were left for about 24 hours in 50% relative humidity to dry. According to Alsalman et al.,[9] this procedure results in higher compressive strength with shorter curing times. Accelerated curing was used to create an adequate number of trial batches in a short time to expedite the development of the preferred mixture proportions; however, after trial batching was completed, a different curing regimen was used to report the compressive strengths for the final mixtures at 1, 28, and 56 days. That curing regimen consisted of 16 hours in the mold and 8 hours in a 140°F water tank followed by moist curing in 73.5°F ± 3.5°F (23.0°C ± 2.0°C) water storage tanks until the testing time. All of the compressive strength tests were conducted using 3 × 6 in. (75 × 150 mm) concrete cylinders. The UHPC in this study required a different curing regimen, which is described later.

The ends of all concrete cylinders were grinded before testing. The reported compressive strength was the mean compressive strength for three cylinders, with a standard deviation of 0.3 to 0.8 for 17 ksi (117 MPa) compressive strength UHSC (UHSC-17) and 20 ksi (138 MPa) compressive strength UHSC (UHSC-20). The standard deviation for the compressive strength results of the UHPC was 0.6 to 1.1.

Development of UHSC-17

Trial mixtures for UHSC-17 were batched in a 2.0 ft^3 (0.057 m^3) drum mixer. Before they were mixed, the fine and coarse aggregates were oven dried to eliminate any inconsistency associated with variations in moisture content. The mixtures were varied by changing the water-binder ratios *w/b*, HRWRA dosage, and cement, fly ash, silica fume, and coarse aggregate contents. Given the many variables considered and the desire to test the compressive strength at 56 days, it took more than a year to reach the final material proportions that produced the desired strength, consistency, and workability. The purpose of testing the compressive strength at 56 days was to investigate the long-term gain in concrete strength due to the use of fly ash.

Because silica fume is so much more costly than portland cement and fly ash, the first stage of the mixture development was to obtain the highest strength possible without using silica fume. **Table 2** shows selected mixture proportions that led to high compressive strength without silica fume. It was possible to achieve a compressive strength of 17.6 ksi (121 MPa) using 900 lb/yd^3 (534 kg/m^3) of cement, 350 lb/yd^3 (208 kg/m^3) of fly ash, and no silica fume. The 17.6 ksi compressive strength was achieved after 28 days of moist curing at 70°F (21°C). The workability was tested by measuring the slump flow per the *Standard Test Method for Slump Flow of Self-Consolidating Concrete* ASTM C1611[15] (**Fig. 2**). Through proper balancing of the mixture proportions, a 35 in. (889 mm) spread was achieved, which gave excellent workability while maintaining good consistency.

Development of UHSC-20

After achieving the highest compressive strength possible without silica fume, we made several more batches incorporating silica fume to reach a target strength of 20 ksi (138 MPa). In several batches, cement and fly ash content were held constant and the silica fume content was increased by 5% increments from 0% to 15% by cement weight. This allowed investigators to monitor gains in strength as silica fume content increased. Based on the strength and the workability of the mixtures, 130 lb/yd^3 (77.1 kg/m^3) of silica fume was found to give the greatest strength with minimal effect on workability. **Table 3** shows the material proportions for these mixtures.

Table 2. Mixture proportions for selected ultra-high-strength concrete without silica fume

Material	UHSC 1	UHSC 2	UHSC 3	UHSC 4
Binder, lb/yd³	1050	1000	1150	1250
Cement, lb/yd³	900	700	800	900
Fly ash, lb/yd³	150	300	350	350
Silica fume, lb/yd³	0	0	0	0
Coarse aggregate, lb/yd³	1200	1200	1200	1200
Fine aggregate, lb/yd³	1579	1558	1447	1300
Water, lb/yd³	262.5	250.0	264.5	287.5
Water-binder ratio *w/b*	0.250	0.250	0.230	0.230
ADVA 455 high-range water-reducing admixture, lb/yd³	37	30	33	35
Spread, in.	23	28	32	35
f'_{ci} at 1 day, ksi	12.70	11.30	12.10	12.30
f'_c at 28 days, ksi	14.50	15.30	16.80	17.60
f'_c at 56 days, ksi	15.10	16.20	17.40	18.10
f'_c at 5 days of heat curing, ksi	14.40	16.60	16.90	17.20

Note: f'_c = design concrete compressive strength at final service conditions; f'_{ci} = design concrete compressive strength at time of transfer of the prestressing force; UHSC = ultra-high-strength concrete. 1 in. = 25.4 mm; 1 lb/yd³ = 0.5933 kg/m³; 1 ksi = 6.895 MPa.

Table 3. Mixture proportions for selected ultra-high-strength concrete with silica fume

Material	UHSC 5	UHSC 6	UHSC 7	UHSC 8	UHSC 9	UHSC 10	UHSC 11
Binder, lb/yd³	1715	1780	1845	1680	1880	1580	1780
Cement, lb/yd³	1300	1300	1300	1200	1400	1300	1300
Fly ash, lb/yd³	350	350	350	350	350	150	350
Silica fume, lb/yd³	65	130	195	130	130	130	130
Coarse aggregate, lb/yd³	900	900	900	900	900	900	0
Fine aggregate, lb/yd³	1040	928	817	1065	842	1244	1812
Water, lb/yd³	343	356	369	336	357.2	316	356
Water-binder ratio *w/b*	0.20	0.20	0.20	0.20	0.19	0.20	0.20
ADVA 455 high-range water-reducing admixture, lb/yd³	37	37	37	37	37	37	37
Spread, in.	35.25	34.0	n.d.	33.0	34.0	30.75	n.d.
f'_{ci} at 1 day, ksi	12.4	13.4	12.9	12.6	13.7	14.1	12.7
f'_c at 28 days, ksi	16.20	18.00	16.70	16.30	18.80	16.70	17.70
f'_c at 56 days, ksi	17.40	18.90	17.10	17.30	20.50	17.50	18.90
f'_c at 5 days of heat curing, ksi	17.80	18.40	18.20	16.80	19.80	18.20	18.30

Note: f'_c = design concrete compressive strength at final service conditions; f'_{ci} = design concrete compressive strength at time of transfer of the prestressing force; n.d. = no data; UHSC = ultra-high-strength concrete. 1 in. = 25.4 mm; 1 lb/yd³ = 0.5933 kg/m³; 1 ksi = 6.895 MPa.

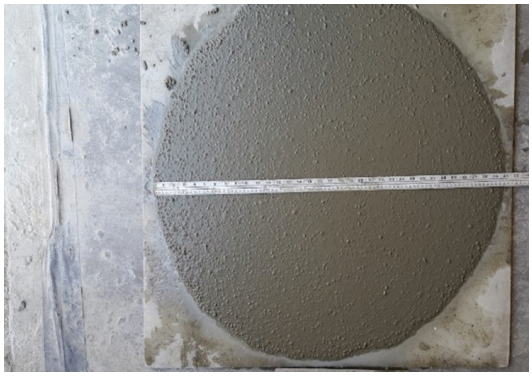

Figure 2. Slump flow for the 17 ksi compressive strength ultra-high-strength concrete. Note: 1 ksi = 6.895 MPa.

A Hobart 5-gal. (19-L) laboratory pan mixer was used to mix the 20 ksi (138 MPa) compressive strength UHSC. This mixer was used instead of the drum mixer that was used for UHSC-17 because the concrete mixtures with higher binder contents and lower water-binder ratios w/*b* could not be mixed efficiently using a small drum mixer. The concrete tended to stick to the drum sides and rotate with the pan for more than 20 minutes with no shearing from the blades.

Type I/II cement, regular gradation sand, ¼ in. (6.4 mm) crushed limestone, silica fume, and Class C fly ash were mixed for 3 minutes, and then water and HRWRA was added gradually. After the water was added, complete mixing took between 3 and 5 minutes. Table 3 highlights different mixture proportions that achieved the greatest strengths, including the 20 ksi (138 MPa) compressive strength UHSC labeled UHSC 9.

The 20 ksi (138 MPa) compressive strength UHSC was achieved using only 130 lb/yd^3 (77.1 kg/m^3) of silica fume,

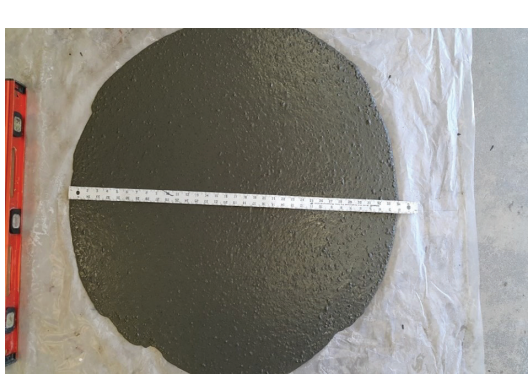

Figure 3. Slump flow for the 20 ksi compressive strength ultra-high-strength concrete. Note: 1 ksi = 6.895 MPa.

an amount that is considered low compared with several similar mixtures in the literature.[1,4,8,10,16] The mixture was very consistent, with a slump flow of 34 in. (864 mm) (**Fig. 3**). The 20 ksi compressive strength was obtained after 56 days of standard moist curing.

Fly ash was a key component in the mixture optimization. Using fly ash reduced mixing time and increased both the ultimate compressive strength and the workability and consistency of the mixture. **Table 4** presents four mixture proportions that have different amounts of fly ash. With a constant water-binder ratios *w*/*b*, using a higher percentage of fly ash increased the binder content, which in turn increased the water content, providing more workability for the mixtures. Increasing the fly ash content from 12% to 36% by cement weight led to an increase in the spread by inverted slump flow from 22 to 35 in. (559 to 889 mm). Comparing UHSC 1 with UHSC 4 in Table 2, it can be seen that at the same cement content, increasing fly ash content from 150 to 350 lb/yd^3 (89 to 208 kg/m^3) led to a 20% increase in the 56-day strength and a 52% increase in the spread as measured by the inverted slump flow test. This finding indicates that fly ash can improve the strength and workability of HSC and UHSC mixtures and should be more widely used when producing such mixtures in precast concrete facilities.

Development of UHPC-24

In addition to the 17 ksi (117 MPa) and 20 ksi (138 MPa) UHSC, we developed a UHPC with a targeted compressive strength of 24 ksi (165 MPa). The UHPC mixture proportions were designed to compare their material use, workability, and ease of production with comparable qualities of the UHSC mixtures. In the UHPC mixtures, no coarse aggregate was used. The trial mixtures were made using Type I/II cement, masonry sand, Class C fly ash, quartz flour, and two types of silica fume. The densified gray silica fume was used in 24 ksi compressive strength UHPC (UHPC-24) and the undensified white silica fume was used in 25 ksi compressive strength UHPC (UHPC-25). The dry materials were added at once and mixed for 5 minutes, then the water and the HRWRA were added gradually, and the mixing continued for an additional 20 minutes in the pan mixer. **Table 5** shows the final mixture proportions for the two UHPC mixtures and the corresponding compressive strength values. The strengths were tested at 2, 28, and 56 days using 3 × 6 in. (75 × 150 mm) concrete cylinders. Twenty-four hours after they were cast, the cylinders were placed in a water tank with a temperature of 140°F (60°C) for 16 hours and then the temperature was raised to 194°F (90°C) for 8 hours. After that, the cylinders were moist cured until the testing time.

UHPC required a longer mixing time and greater mixing energy than were needed to produce UHSC. The mixing time for UHPC was much longer than that for UHSC. It was noted that using a normal gradation sand did not significantly reduce the compressive strength. Other studies reported same results regarding the use of normal gradation sand.[8,9]

Table 4. Mixture proportions of selected ultra-high-strength concrete with different amounts of fly ash

Material	UHSC 12 with 12% fly ash	UHSC 13 with 19% fly ash	UHSC 14 with 27% fly ash	UHSC 15 with 36% fly ash
Binder, lb/yd³	1555	1650	1750	1870
Cement, lb/yd³	1300	1300	1300	1300
Fly ash, lb/yd³	155	250	350	470
Silica fume, lb/yd³	100	100	100	100
Coarse aggregate, lb/yd³	800	800	800	800
Fine aggregate, lb/yd³	1386	1236	1078	889
Water, lb/yd³	311	330	350	374
Water-binder ratio *w/b*	0.20	0.20	0.20	0.20
Spread, in.	22	25	29	35
ADVA 455 high-range water-reducing admixture, lb/yd³	38	38	38	38
f'_c at 56 days, ksi	17.3	18.9	18.6	18

Note: f'_c = design concrete compressive strength at final service conditions; UHSC = ultra-high-strength concrete. 1 in. = 25.4 mm; 1 lb/yd³ = 0.5933 kg/m³; 1 ksi = 6.895 MPa.

Table 5. Final mixture proportions for ultra-high-performance concrete

Material	UHPC-24	UHPC-25
Binder, lb/yd³	1798	1800
Cement, lb/yd³	1450	1400
Fly ash, lb/yd³	145	100
Silica fume, lb/yd³	203	300
Silica flour, lb/yd³	350	350
Coarse aggregate, lb/yd³	0	0
Fine aggregate, lb/yd³	1553	1525
Steel fiber, lb/yd³	197	0
Water, lb/yd³	324	324
Water-binder ratio *w/b*	0.18	0.18
ADVA 455 high-range water-reducing admixture, lb/yd³	55	40
Spread, in.	7	10
f'_{ci} at 2 days, ksi	16.7	17.50
f'_c at 28 days, ksi	21.40	23.10
f'_c at 56 days, ksi	24.20	25.60

Note: f'_c = design concrete compressive strength at final service conditions; f'_{ci} = design concrete compressive strength at time of transfer of the prestressing force; UHPC = ultra-high-performance concrete. 1 in. = 25.4 mm; 1 lb/yd³ = 0.5933 kg/m³; 1 ksi = 6.895 MPa.

The type of silica fume used in the mixtures had a noticeable effect on the workability and the strength of the UHPC. The UHPC with the densified gray silica fume required longer mixing times and had lower compressive strength and lower workability compared with the UHPC with the undensified white silica fume. To further investigate the differences and to share some knowledge about the two types of silica fume, investigators conducted X-ray fluorescence analysis and scan-

ning electron microscopy (SEM) imaging on both silica fumes. **Table A.1** in Appendix A shows the proportions of all types of oxides in each silica fume found via X-ray fluorescence analysis. Notably, the undensified white silica fume contained 4.61% of zirconium dioxide (ZrO_2) whereas ZrO_2 was not detected in the densified gray silica fume. Some studies have found that ZrO_2 increases the strength of the concrete.[17,18] Also, compared with the densified gray silica fume, the undensified white silica fume contained more silica (SiO_2), which in turn led to greater strength.[19] SEM imaging was performed on the silica fume particles to see the differences in particle size and shape. **Figure A.1** in Appendix A shows that the gray silica fume tended to have regular spherically shaped particles whereas the white silica fume particle had an irregular shape and seemed to agglomerate in a weak mass that easily broke out to smaller particles. It is out of the study's scope to fully discuss the effects of silica fume's particle size, shape, and chemical composition on fresh and hardened concrete properties. The densified gray silica fume was used throughout the study because of its availability in the local markets.

Evaluation of design parameters

The equations in the American Association of State Highway and Transportation Officials' *AASHTO LRFD Bridge Design Specifications*[14] for MOE, flexural strength, creep, and shrinkage were developed for HSC and may not accurately predict UHSC properties. Therefore, accurate predictions of these mechanical properties require experimental testing. The design of precast and prestressed concrete girders requires knowledge of the average shrinkage strain and the creep coefficient, as well as proper prediction of the MOE and flexural strength. We determined these parameters experimentally and compared them with the design values based on equations in the AASHTO LRFD specifications.

Modulus of elasticity

The accuracy of MOE predictions determines the accuracy of elastic deformation and prestress loss predictions. The compressive strength, MOE, and unit weight were measured for the three mixtures (UHSC-17, UHSC-20, and UHPC-24). Testing was conducted at 2, 7, 28, and 56 days of age using three 3 × 6 in. (75 × 150 mm) concrete cylinders to measure the compressive strength and three 4 × 8 in. (100 × 200 mm) concrete cylinders for the MOE. A compressometer ring equipped with linear variable displacement transducers was used to measure the MOE. **Figure 4** shows the relationship between concrete compressive strength and MOE using Eq. (5.4.2.4-1) from the 2017 AASHTO LRFD specifications[14] and Eq. (5) from Graybeal.[20]

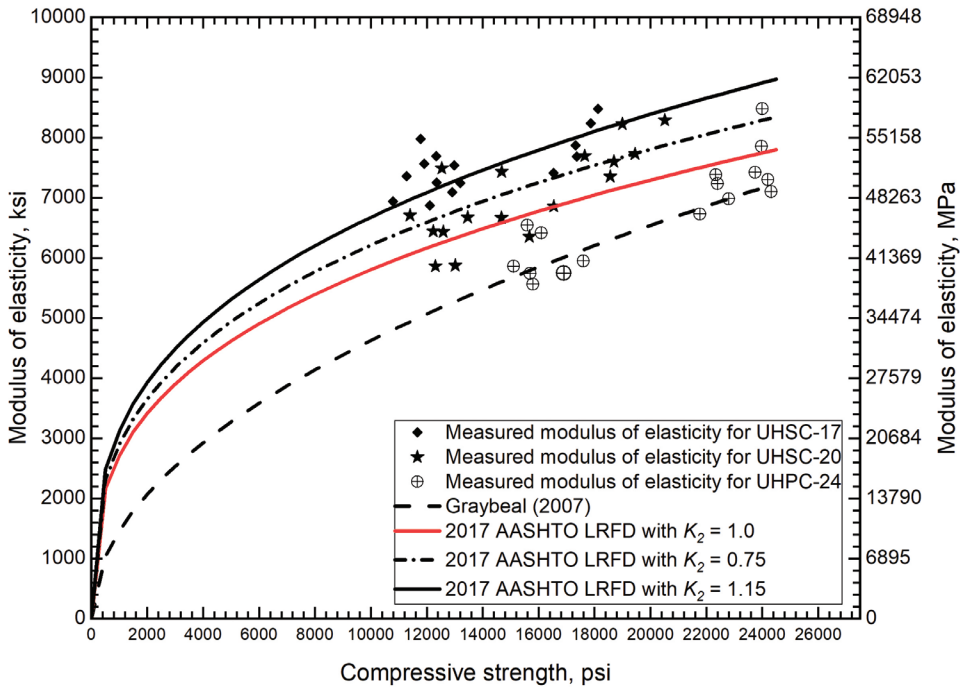

Figure 4. Comparison of the measured modulus of elasticity with the predicted values. Note: 2017 AASHTO LRFD = eighth edition of the American Association of State Highway and Transportation Officials' *AASHTO LRFD Bridge Design Specifications*; K_2 = calibration factor for modulus of elasticity; UHPC-24 = 24 ksi compressive strength ultra-high-performance concrete; UHSC-17 = 17 ksi compressive strength ultra-high-strength concrete; UHSC-20 = 20 ksi compressive strength ultra-high-strength concrete. 1 psi = 6.895 kPa; 1 ksi = 6.895 MPa.

$$E_c = 120{,}000 K_1 K_2 w_c^{2.0} f_c'^{0.33} \quad \text{(AASHTO LRFD 5.4.2.4-1)}$$

where

E_c = modulus of elasticity of concrete at erection

f_c' = design concrete compressive strength at final service conditions

K_1 = correction factor for source of aggregates

K_2 = calibration factor for modulus of elasticity

w_c = unit weight (density) of concrete

$$E_c = 1705.09 K_1 K_2 \left(\frac{w_C}{1000}\right)^{2.0} f_c'^{0.33} \quad \text{(Graybeal 5)}$$

$$E_c = 46{,}200\sqrt{f_c'}$$

where f_c' is in psi

$$E_c = 3840\sqrt{f_c'}$$

where f_c' is in MPa

The design MOE was plotted using 150.2 lb/ft^3 (2406 kg/m^3) for the unit weight, and calibration factor K_2 values ranging from 1.0 to 1.15. The 150.2 lb/ft^3 unit weight was the average value of several tests conducted during the mixture proportioning process. The calibration factor K_2 is used to bring the estimated MOE closer to the measured values. Figure 4 indicates that AASHTO's Eq. (5.4.2.4-1) provides a good estimation of the initial MOE for the UHSC-17 and UHSC-20 mixtures when the K_2 value is set to 1.15 for UHSC-17 and 0.75 for UHSC-20. The final MOEs for UHSC-17 and UHSC-20 can be found using the same equations with K_2 values equal to 0.75. Graybeal's Eq. (5) shows good agreement with the MOE of UHPC-24. The correction factor for source of aggregates K_1 value was set to 1.0 for all mixtures.

Flexural strength

Six 4 × 4 × 20 in. (100 × 100 × 510 mm) prisms were made from each mixture to measure flexural strength. The prisms were tested in a third-point loading according to the *Standard Test Method for Flexural Strength of Concrete (Using Simple Beam with Third-Point Loading),* ASTM C78[21] (**Fig. 5**). Because steel fiber increases flexural strength, another six prisms were made for each mixture with steel fibers added to the mixtures to evaluate the increase in the flexural strength due to the addition of steel fiber. The additional prisms contained 1.5% (by volume) of steel fiber. Prisms cast with UHSC-17 had Force 1050 steel fiber by Sika Fiber added and are designated UHSC-SF-17. Prisms cast with UHSC-20 and UHPC-24 had Dramix OL 13/.20 steel fiber by Bekaert added and are designated UHSC-SF-20 and UHPC-SF-24, respectively. **Figure 6** reports the average flexural strength for the mixtures with and without steel fiber after 56 days of moist curing.

Steel fiber increased the flexural strength for the UHSC-SF-17, UHSC-SF-20, and UHPC-SF-24 mixtures by 22%, 96%, and 300%, respectively, compared with their base mixtures without steel fiber. This finding demonstrates the importance of steel fiber in achieving mixtures with compressive strengths of 20 ksi (138 MPa) or higher. It is important to point out that for the prisms without steel fiber, the flexural strength of the UHSC-17 mixture is 64% greater than that of UHSC-20 and 37% higher than that of UHPC-24. This

Test setup

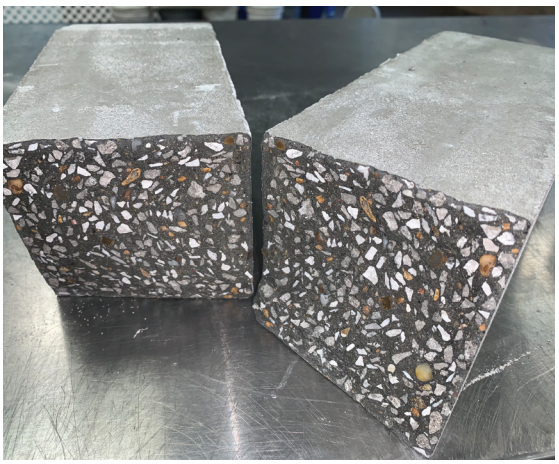

Test setup

Figure 5. Flexural strength test.

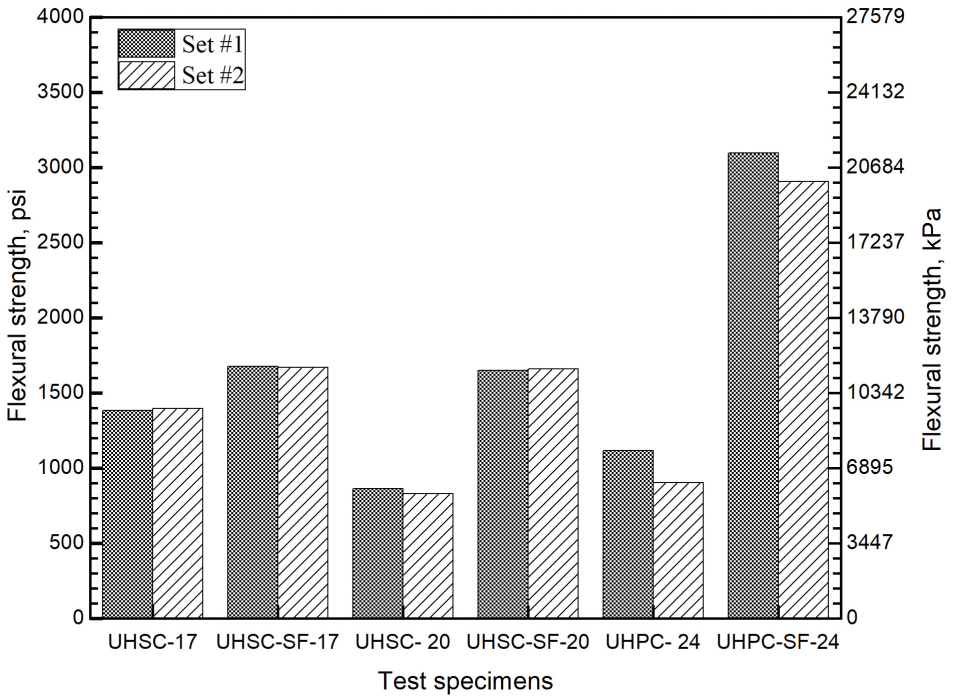

Figure 6. Average flexural strength for the mixtures with and without steel fiber. Note: UHPC-24 = 24 ksi compressive strength ultra-high-performance concrete; UHPC-SF-24 = 24 ksi compressive strength ultra-high-performance concrete with steel fibers; UHSC-17 = 17 ksi compressive strength ultra-high-strength concrete; UHSC-20 = 20 ksi compressive strength ultra-high-strength concrete; UHSC-SF-17 = 17 ksi compressive strength ultra-high-strength concrete with steel fibers; UHSC-SF-20 = 20 ksi compressive strength ultra-high-strength concrete with steel fibers.

Table 6. The measured flexural strength of concrete as a percentage of the square root of compressive strength

Mixture	Flexural strength, ksi
UHSC-17	$0.32\sqrt{f'_c}$
UHSC-SF-17	$0.39\sqrt{f'_c}$
UHSC-20	$0.19\sqrt{f'_c}$
UHSC-SF-20	$0.37\sqrt{f'_c}$
UHPC-24	$0.22\sqrt{f'_c}$
UHPC-SF-24	$0.63\sqrt{f'_c}$

Note: f'_c = design concrete compressive strength at final service conditions in ksi; UHPC-24 = 24 ksi compressive strength ultra-high-performance concrete; UHPC-SF-24 = 24 ksi compressive strength ultra-high-performance concrete with steel fibers; UHSC-17 = 17 ksi compressive strength ultra-high-strength concrete; UHSC-SF-17 = 17 ksi compressive strength ultra-high-strength concrete with steel fibers; UHSC-20 = 20 ksi compressive strength ultra-high-strength concrete; UHSC-SF-20 = 20 ksi compressive strength ultra-high-strength concrete with steel fibers. 1 ksi = 6.895 MPa.

finding indicates that the presence of crushed limestone increases the tensile capacity of the concrete. Bayasi and Zhou[22] reported that increasing the coarse aggregate content increases the flexural strength. Aggregate can bridge the cracks in the matrix under flexural loads.

The flexural strength for normal-strength concrete is between $0.24\sqrt{f'_c}$ and $0.37\sqrt{f'_c}$ where f'_c is measured in ksi.[14] Section 5.4.2.6 of the AASHTO LRFD specifications[14] states that the flexural strength for concrete with compressive strength up to 15 ksi (103 MPa) can be taken as $0.24\sqrt{f'_c}$. **Table 6** presents the flexural strength in relation with the square root of compressive strength.

The reported flexural strength of the UHPC in this study includes the additional postcracking strength achieved due to the inclusion of fibers. For the other mixtures in this study, the concrete failed in flexure as the first crack appeared. Steel fibers bridge the cracks and allow the concrete to resist a greater load after the initial crack until the steel fiber fails.

Shrinkage strain

The developed mixtures were expected to undergo high shrinkage strain due to the relatively high binder content.

Therefore, the shrinkage strain was measured and compared with results from Eq. (5.4.2.3.3-1) in the AASHTO LRFD specifications.[14] Shrinkage strains were monitored for the UHSC-17, UHSC-20, and UHPC-24 mixtures. Three 4 × 4 × 11¼ in. (100 × 100 × 286 mm) prisms were used for each mixture to measure the change in length with time according to the *Standard Test Method for Length Change of Hardened Hydraulic-Cement Mortar and Concrete*, ASTM C157.[23] Twenty-four hours after casting, the prisms were demolded, measured in a length comparator, and stored in lime-saturated water at 73°F ± 3°F (23°C ± 1.5°C) for 28 days. The prisms were then removed from the water storage, wiped with a damp cloth, and measured for the second comparator readings. Following 28 days of curing, readings for each prism were taken at 4, 7, 14, and 28 days and then monthly for approximately 1 year.

Figure 7 compares the measured shrinkage strain with the predicted values. The design shrinkage strain ε_{sh} was calculated per AASHTO LRFD Eq. (5.4.2.3.3-1) and correction factors for concrete strength, ambient humidity, volume-to-surface area ratio, and time as follows:

$$\varepsilon_{sh} = k_s k_{hs} k_f k_{td} 0.48 \times 10^{-3} \quad \text{(AASHTO LRFD 5.4.2.3.3-1)}$$

where

$$k_{hs} = (2 - 0.14H) \quad \text{(AASHTO LRFD 5.4.2.3.3-2)}$$

k_s = $1.45 - 0.13(V/S) \geq 1.0$

$$k_f = \frac{5}{1 + f'_{ci}} \quad \text{(AASHTO LRFD 5.4.2.3.2-4)}$$

$$k_{td} = \frac{t}{61 + 4f'_{ci} + t} \quad \text{(AASHTO LRFD 5.4.2.3.2-5)}$$

k_{hs} = shrinkage correction factor for ambient humidity

k_s = factor for the effect of the volume-to-surface area ratio of the component

k_f = correction factor for the effect of concrete strength

k_{td} = time development factor

H = relative humidity

V/S = volume-to-surface area ratio

f'_{ci} = design concrete compressive strength at time of transfer of the prestressing force, ksi

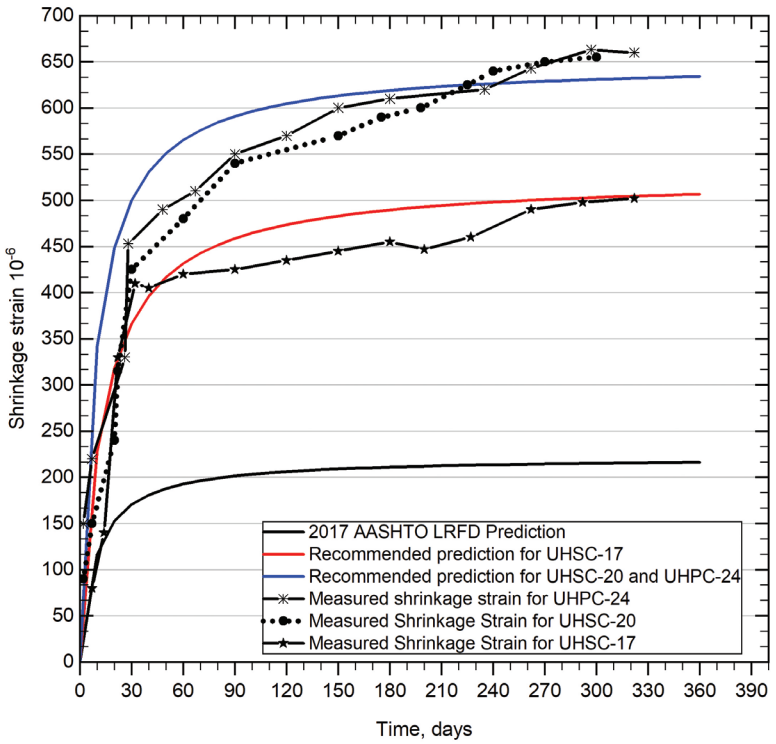

Figure 7. Comparison of the measured shrinkage strain over time with the design values from the eighth edition of the American Association of State Highway and Transportation Officials' *AASHTO LRFD Bridge Design Specifications* for two concrete mixtures. Note: 2017 AASHTO LRFD = eighth edition of the American Association of State Highway and Transportation Officials' *AASHTO LRFD Bridge Design Specifications*; UHPC-24 = 24 ksi compressive strength ultra-high-performance concrete; UHSC-17 = 17 ksi compressive strength ultra-high-strength concrete; UHSC-20 = 20 ksi compressive strength ultra-high-strength concrete.

t = age of concrete between the end of curing and the time to consider shrinkage effect, days

Figure 7 indicates that the procedure in the AASHTO LRFD specifications[14] underestimates the shrinkage strain for the UHSC mixtures. This finding was expected because the AASHTO equations were developed and verified based on measured shrinkage strains of HSC.[24] In this study, modifications were made to the procedure in the AASHTO LRFD specifications to provide a prediction guideline for the shrinkage strain of UHSC. The modifications included increasing the basic concrete strain from 0.48×10^{-3} to 0.58×10^{-3} for UHSC-17 and to 0.64×10^{-3} for UHSC-20 and UHPC-24. The correction factor for concrete strength k_f was increased to accommodate the difference in the strength between the HSC and UHSC. Using the modified procedure results in proper estimation of the concrete strain (Fig. 7). The following equations summarize the proposed modifications to the procedure in the AASHTO LRFD specifications for UHSC:

$$\varepsilon_{sh} = k_s\, k_{hs}\, k_f\, k_{td}\, 0.58 \times 10^{-3} \quad \text{for UHSC-17}$$

$$\varepsilon_{sh} = k_s\, k_{hs}\, k_f\, k_{td}\, 0.64 \times 10^{-3} \quad \text{for UHSC-20 and UHPC-24}$$

$$k_f = \frac{11}{1 + f'_{ci}} \quad \text{for each of the three mixtures}$$

Creep strain

The creep coefficient, which is the ratio of the creep strain to the elastic strain, is used in design calculations to account for the creep of concrete. In this study, the creep coefficient was monitored for the UHSC-17 and UHSC-20 mixtures for 10 months. The capacity of the creep frame was not high enough to measure the creep for UHPC-24. The collected creep strain data were used to assess the applicability of the equations in the AASHTO LRFD specifications[14] for predicting the creep coefficient for the developed UHSC mixtures.

Creep tests were performed on 4 × 8 in. (100 × 200 mm) concrete cylinders made from the UHSC-17 and UHSC-20 mixtures (**Fig. 8**). Two cylinders were tested for compressive strength, two were kept unloaded to measure the shrinkage strain, and two to four cylinders were loaded in the creep frame. Steel frames were assembled with D2-type springs and a hydraulic ram to apply a constant load on the concrete cylinders. The creep specimens were loaded to 40% of their average compressive strength measured at the time of loading according to the *Standard Test Method for Creep of Concrete in Compression,* ASTM C512/C512M.[25] The compressive strengths at loading were 12.91 and 14.1 ksi (89 and 97.2 MPa) for the UHSC-17 and UHSC-20 cylinders, respectively. Concrete creep strains were monitored using the detachable mechanical strain gauge and a reference disk glued on four sides at 90-degree increments around the cylinders.

Figure 9 compares the measured creep coefficients with the predictions derived from the AASHTO LRFD specifications. UHSC-17 experienced less creep strain than UHSC-20 during the period measured. This finding was expected because UHSC-17 had a higher amount of coarse aggregate and lower binder content than UHSC-20. Coarse aggregate provides a higher resistance to deformation than the cement paste. For UHSC-17, the measured creep coefficient was 20% less than the predicted value based on the AASHTO LRFD specifications. For UHSC-20, the measured creep coefficient was 15% higher than the prediction.

Figure 8. Loaded concrete cylinders for creep tests in the environmental chamber.

Girder design proof of concept

The flexural capacity of a prestressed concrete girder is mainly determined by the number of prestressing strands that can be placed in the bottom flange of the girder cross section. The number of strands is primarily limited by the allowable concrete stresses at the girder ends and at the midspan. Increasing the number of prestressing strands induces greater concrete stresses. These concrete stresses must be within specified limits to prevent concrete failure during transfer of prestress and during service. Using UHSC in bridge girders increases the allowable stress limits so that more strands may be safely placed in the cross section. Using a larger number of strands allows for longer spans or fewer girders for a given span. Taylor et al.[26] used the properties of UHPC and redesigned two existing bridges made with high-performance concrete girders. The study found that the required volume of girder concrete could be reduced by up to 40% if UHPC were used in the design.

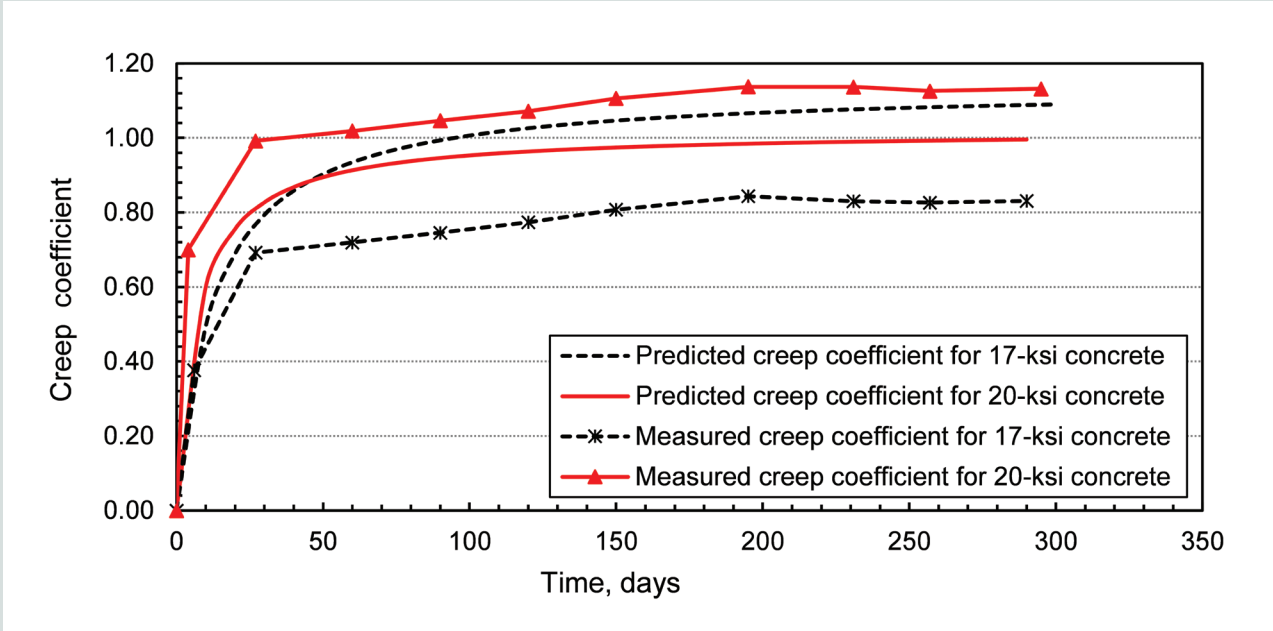

Figure 9. Comparison of the measured creep coefficient over time with the design values from the eighth edition of the American Association of State Highway and Transportation Officials' *AASHTO LRFD Bridge Design Specifications* for two concrete mixtures. Note: AASHTO LRFD = eighth edition of the American Association of State Highway and Transportation Officials' *AASHTO LRFD Bridge Design Specifications*. 1 ksi = 6.895 MPa.

A 300 ft (91.4 m) long bridge girder was designed for flexure as a proof of concept to quantify the competitive advantages of using UHSC in bridge girders. A prototype girder cross section was established based on several iterations to obtain maximized span length within specified concrete stress limits. All the dimensions in this cross section were found to produce the maximum moment of inertia with the least self-weight possible. A typical bridge configuration was presumed to be a four-lane bridge that was 75 ft (23 m) wide, including a 1.5 ft wide (0.46 m wide) parapet. The superstructure consisted of nine simple-span prestressed concrete girders. The girders were spaced at 8.5 ft (2.6 m) on center and topped with a 7 in. thick (180 mm thick) reinforced concrete deck. Given the large concrete stresses at the girder ends, the strands were harped at 0.4 times the span, measured from the ends. **Figure 10** shows the cross-section details and the distribution of the strands at the

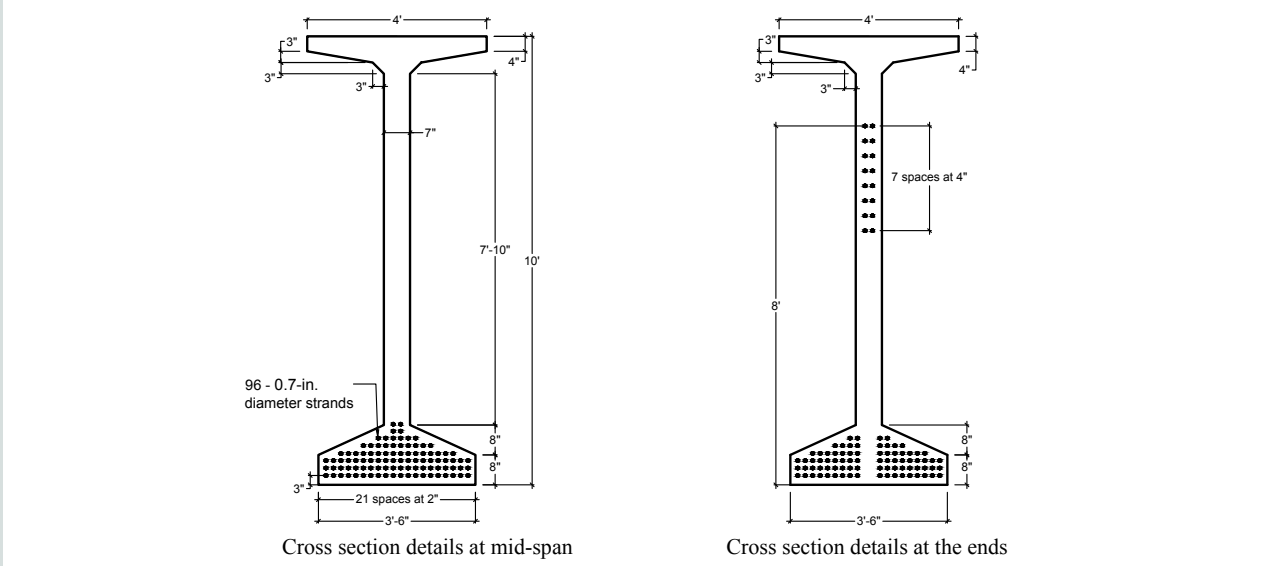

Figure 10. Girder cross section needed to span 296 ft. Note: " = 1 in. = 25.4 mm; ' = 1 ft = 0.305 m.

girder ends and at midspan. The 10 ft (3.05 m) girder depth was the minimum depth needed to reduce the concrete stresses at the bottom flange at midspan.

Three girders were designed using the three concrete mixtures that were developed in this study. The modulus of elasticity, shrinkage, and creep were predicted based on the recommendations presented earlier in this paper. Appendix B presents the material properties, cross-section properties, bridge geometry, and design moments used in the flexural design of the three girders.

Table 7 presents the critical concrete stresses at the top and bottom fibers of the girders, in addition to the nominal moment capacity, camber, and prestress losses. At the time of transfer, the stresses at the top and bottom concrete fibers at transfer length governed the design and were calculated using Eq. (1) and Eq. (2). For service loads, the maximum compressive stresses were calculated under the Service I limit state using Eq. (3) and the maximum tensile stresses were checked under the Service III limit state using Eq. (4) according to the load combinations in Section 3.4.1 of the AASHTO LRFD specifications.[14] The erection camber was estimated based on the multiplier method in Section 8.7.1 of the *PCI Bridge Design Manual*.[27] Prestress losses were estimated using the refined estimates method in the AASHTO LRFD specifications. The factored flexural resistance was calculated according to Section 5.6.3.1 of the AASHTO LRFD specifications.

$$f_{t,transfer} = \frac{P_{pi}}{A_{Ti}} - \frac{P_{pi}e_{ti}}{S_{ti}} + \frac{M_{g,transfer}}{S_{ti}} \quad (1)$$

where

$f_{t,transfer}$ = concrete stress at top of girder at transfer length at the time of transfer

P_{pi} = initial prestressing force immediately before transfer

A_{Ti} = transformed area of girder section at transfer

e_{ti} = distance between centers of gravity of strands and concrete section at time of transfer

S_{ti} = section modulus for the top extreme fiber of the girder section at transfer

$M_{g,transfer}$ = moment at transfer length section due to girder weight, based on total girder length

$$f_{b,transfer} = \frac{P_{pi}}{A_{Ti}} + \frac{P_{pi}e_{ti}}{S_{bi}} - \frac{M_{g,transfer}}{S_{bi}} \quad (2)$$

where

$f_{b,transfer}$ = concrete stress at bottom of girder at transfer length at the time of transfer

S_{bi} = section modulus for bottom extreme fiber of the girder section at transfer

$$f_{t,service} = \frac{P_f}{A_{Tf}} - \frac{P_f e_{tf}}{S_{tf}} + \frac{M_{DC1} + M_{DC2}}{S_{tf}} + \frac{M_{DC3} + M_{DW}}{S_{tfC}} + \frac{\left(M_{(LL+IM)HL93}\right)}{S_{tfC}} \quad (3)$$

where

$f_{t,service}$ = concrete stress at top of girder at transfer length at time of service

P_f = effective force in prestressing strands after all losses

A_{Tf} = transformed area of girder section at time of service

S_{tf} = section modulus for the top extreme fiber of the composite section at service stage

e_{tf} = distance between centers of gravity of strands and concrete section at time of service

M_{DC1} = unfactored moment due to girder self-weight

M_{DC2} = unfactored moment due to slab and haunch weight

M_{DC3} = unfactored moment due to barrier weight

M_{DW} = unfactored moment due to future wearing surface

Table 7. Critical concrete stresses and moment capacity for three bridge girders

Mixture	Clear span length, ft	ϕM_n, kip-ft	Critical stresses at midspan, ksi		Critical stresses at transfer length, ksi		Erection camber, in.	Final losses, ksi
			Top	Bottom	Top	Bottom		
UHSC-17	296	61,328	7.020	-1.307	1.29	4.41	4.19	23.41
UHSC-20	296	61,882	7.107	-1.273	1.30	4.43	4.03	19.52
UHPC-24	296	61,328	6.769	-0.959	1.28	4.34	4.34	19.35

Note: M_n = flexural capacity; UHSC-17 = 17 ksi compressive strength ultra-high-strength concrete; UHSC-20 = 20 ksi compressive strength ultra-high-strength concrete; UHSC-24 = 24 ksi compressive strength ultra-high-strength concrete; ϕ = resistance factor. 1 in. = 25.4 mm; 1 ft = 0.303 m; 1 kip-ft = 1.356 kN-m; 1 ksi = 6.895 MPa.

S_{tfC} = section modulus for the top extreme fiber of the composite section

$M_{(LL+IM)HL93}$ = maximum service live load moment at midspan

$$f_{b,service} = \frac{P_f}{A_{Tf}} + \frac{P_f e_{tf}}{S_{bf}} - \frac{M_{DC1} + M_{DC2}}{S_{bf}} - \frac{M_{DC3} + M_{DW}}{S_{bfC}} - \frac{\left(M_{(LL+IM)HL93}\right)}{S_{bfC}} \quad (4)$$

where

$f_{b,service}$ = concrete stress at bottom of girder at transfer length at time of service

S_{bf} = section modulus for the bottom extreme fiber of the composite section at service stage

S_{bfC} = section modulus for the bottom extreme fiber of the composite section

For the three girders, the compressive stresses due to the sum of the effective prestress, permanent loads, and maximum live load were less than the $0.45 f'_c$ limit in Table 5.9.2.3.2a-1 in the AASHTO LRFD specifications. However, the tensile stresses at the bottom of the girder at midspan were the most critical and governed the prestressing force requirement and thus the number of prestressing strands. These stresses were calculated under the Service III limit state, which included the moment due to the full dead load and 80% of the HL-93 vehicular live load according to Table 3.4.1-1 in the AASHTO LRFD specifications.

The AASHTO LRFD specifications limits the tensile stress in Table 5.9.2.3.2b-1 to $0.19\sqrt{f'_c}$. However, this limit is applicable for concrete compressive strengths up to 15 ksi (103 MPa). Therefore, the design concrete stresses in the bottom fiber of the girder were compared with the average measured flexural strength from Table 6.

Figure 11 shows how the tensile stress at the bottom of the girder increases as span length increases. At a span length of 275 ft (83.8 m), the proposed girder design resulted in a tensile stress close to zero, which indicates a balance between the applied moment and the resisting moment from the prestressing force. It is important to note that there were no noticeable decreases in the concrete stresses at the bottom fiber when the compressive strength increased from 17 to 24 ksi (117 to 165 MPa). However, higher compressive strength increases the allowable limits of the tensile stresses, which means longer spans can be designed.

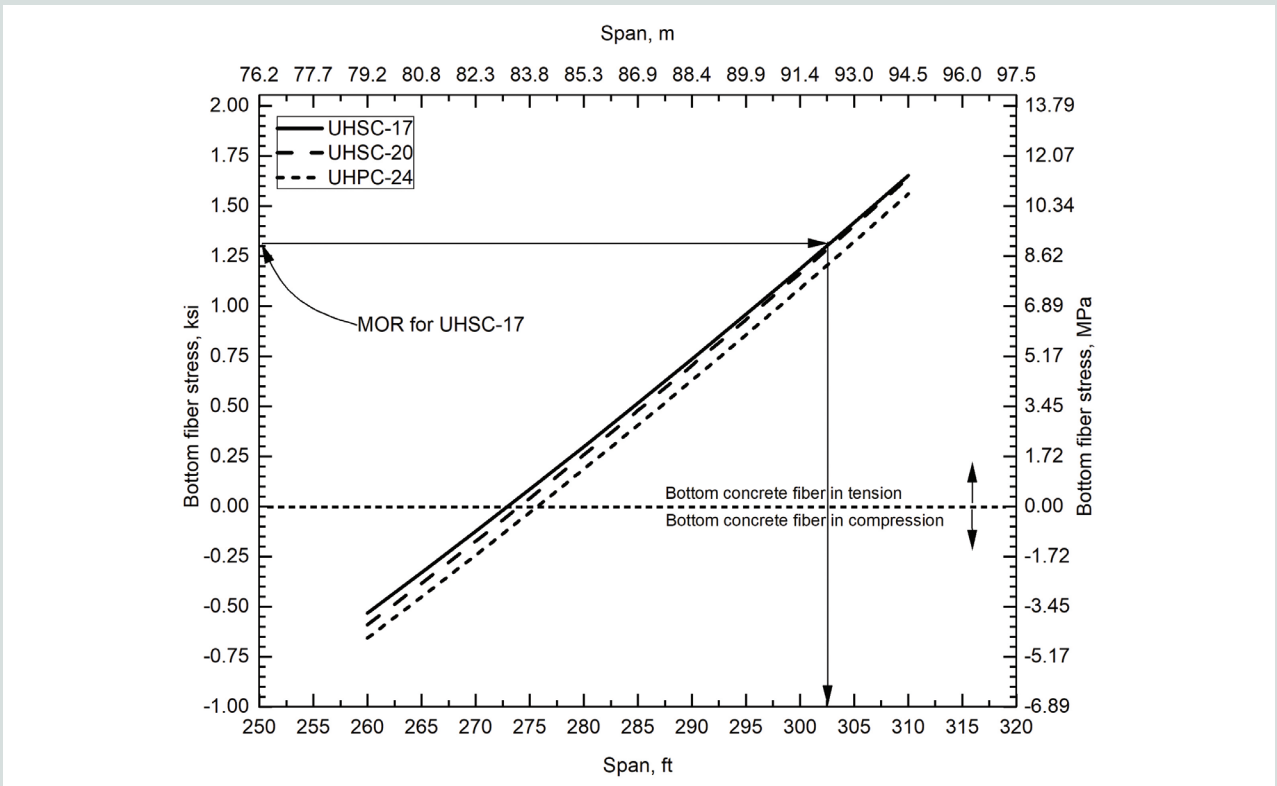

Figure 11. Girder span compared with the concrete stresses in the bottom fiber at midspan under the Service III limit state. Note: MOR = modulus of rupture; UHPC-24 = 24 ksi compressive strength ultra-high-performance concrete; UHSC-17 = 17 ksi compressive strength ultra-high-strength concrete; UHSC-20 = 20 ksi compressive strength ultra-high-strength concrete.

For the mixtures without steel fiber, the measured flexural strength can be compared directly to the stress limits in the AASHTO LRFD specifications because the tests were done according to ASTM C78.[21] The average measured flexural strength for UHSC-17 was 1.319 ksi (9.095 MPa). That is greater than 1.307 ksi (9.012 MPa), which is the bottom concrete fiber stress at midspan for girders designed with UHSC-17 provided in Table 7. Figure 11 shows that engineers can design a 300 ft (91.4 m) long bridge girder using the UHSC-17 mixture, which does not contain steel fiber or silica fume and has less cement content than UHSC-20 and UHPC. This can reduce the cost of the mixture and eliminate the extra efforts required when using fiber-reinforced concrete containing large amounts of silica fume. On the other hand, UHSC-20 and UHPC-24 mixtures without steel fiber showed less flexural strength than UHSC-17 (Fig. 6). Therefore, steel fiber would be required in UHSC-20 and UHPC-24 to reach the same span length of girder design as UHSC-17.

It should be noted that the concrete stresses are not the only parameters limiting the design spans for bridge girders. Additional considerations should be given to the girder stability and stresses during plant handling, hauling, and erection.

Conclusion

The objective of this project was to develop UHSC mixtures that can be produced easily and economically in precast concrete facilities without modifications to typical equipment. It can be concluded that mixtures with compressive strengths up to 20 ksi (138 MPa) have the potential to be implemented in large-scale projects and precast concrete facilities. The UHPC mixture developed in this paper is unlikely to be implemented easily because of its challenging mixing requirements. Standard UHPC mixtures also require high binder contents, low water-binder ratios *w*/*b*, and a large amount of silica powder. Such UHPC mixtures require longer mixing times and more mixing energy, and produce concrete with lower flowability and workability than the UHSC mixtures developed in this study. The curing procedure for UHSC is also much more practical than that needed for UHPC. The UHSC mixtures in this study will require 16 to 24 hours of steam curing to achieve 60% of the 28-day compressive strength required for prestress transfer. This curing period is already used in the production of most concrete members cast with HSC. The paper also demonstrates a successful flexural and allowable stress design for a prestressed concrete girder bridge with a clear span length of up to 296 ft (90.2 m).

Acknowledgments

The work in this paper was sponsored by PCI through the 2018 Dennis R. Mertz Bridge Research Fellowship. Thank you to the project advisory group, including Roger Becker, Lee Lawrence, J. P. Binard, Roy Eriksson, and Finn Hubbard. The authors are thankful to Dylan Scott and Brian Green at the U.S. Army Engineer Research and Development Center/U.S. Army Corps of Engineers for providing the silica flour for the project. Special thanks to Boral Resources, GCP Applied Technologies, Bekaert Corp., Sika Corp., and APAC-Central Inc. in Van Buren, Ark.

References

1. Khaloo, A. R., H. Karimi, S. Asadollahi, and M. Dehestani. 2017. "A New Mixture Design Method for Ultra-High-Strength Concrete." *ACI Materials Journal* 114 (2): 215–224. https://doi.org/10.14359/51689475.

2. Tadros, M. K., and G. Morcous. 2009. *Application of Ultra-High Performance Concrete to Bridge Girders*. Lincoln, NE: Mid-America Transportation Center. https://digitalcommons.unl.edu/cgi/viewcontent.cgi?referer=&httpsredir=1&article=1046&context=matcreports.

3. Russell, H. G., and B. A. Graybeal. 2013. *Ultra-High Performance Concrete: A State-of-the-Art Report for the Bridge Community*. FHWA-HRT-13-060. McLean, VA: FHWA (Federal Highway Administration). https://www.fhwa.dot.gov/publications/research/infrastructure/structures/hpc/13060.

4. Giesler, A. J., S. B. Applegate, and B. D. Weldon. 2016. "Implementing Nonproprietary, Ultra-High-Performance Concrete in a Precasting Plant." *PCI Journal* 61 (6): 68–80. https://doi.org/10.15554/pcij61.6-03.

5. Abbas, S., M. Nehdi, and M. Saleem. 2016. "Ultra-High Performance Concrete: Mechanical Performance, Durability, Sustainability and Implementation Challenges." *International Journal of Concrete Structures and Materials* 10 (3): 271–295. https://doi.org/10.1007/s40069-016-0157-4.

6. Al-Omaishi, N., M. K. Tadros, and S. J. Seguirant. 2009. "Elasticity Modulus, Shrinkage, and Creep of High-Strength Concrete as Adopted by AASHTO." *PCI Journal* 54 (3): 44–63. https://doi.org/10.15554/pcij.06012009.44.63.

7. Tadros, M. K., D. Gee, M. Asaad, and J. Lawler. 2020. "Ultra-High-Performance Concrete: A Game Changer in the Precast Concrete Industry." *PCI Journal* 65 (3): 33–36. https://doi.org/10.15554/pcij65.3-06.

8. Weldon, B. D., D. V. Jauregui, C. M. Newtson, C. W. Taylor, K. F. Montoya, and S. Allena. 2010. *Feasibility Analysis of Ultra High Performance Concrete for Prestressed Concrete Bridge Applications*. NM09MSC-01. Santa Fe, NM: New Mexico Department of Transportation Research Bureau. https://rosap.ntl.bts.gov/view/dot/24640.

9. Alsalman, A., C. N. Dang, and W. M. Hale. 2017. "Development of Ultra-High Performance Concrete with Locally Available Materials." *Construction and Building Materials* 133: 135–145. https://doi.org/10.1016/j.conbuildmat.2016.12.040.

10. Graybeal, B. *Development of Non-Proprietary Ultra-High Performance Concrete for Use in the Highway Bridge Sector*. FHWA-HRT-13-100. McLean, VA: FHWA.

11. Binard, J. P. 2017. "UHPC: A Game-Changing Material for PCI Bridge Producers." *PCI Journal* 62 (2): 34–46. https://doi.org/10.15554/pcij62.2-01.

12. Voo, Y. L., W. K. Poon, and S. J. Foster. 2010. "Shear Strength of Steel Fiber-Reinforced Ultrahigh-Performance Concrete Beams without Stirrups." *Journal of Structural Engineering* 136 (11): 1393–400. https://doi.org/10.1061/(ASCE)ST.1943-541X.0000234.

13. Rao Tadepalli, P., N. Hoffman, T. T. C. Hsu, and Y. L. Mo. 2011. *Steel Fiber Replacement of Mild Steel in Prestressed Concrete Beams*. FHWA/TX-09/0-5255-2;0-5255-2. Houston, TX: Department of Civil and Environmental Engineering, Cullen College of Engineering University of Houston. https://rosap.ntl.bts.gov/view/dot/18608.

14. AASHTO (American Association of State Highway and Transportation Officials). 2017. *AASHTO LRFD Bridge Design Specifications.* 8th ed. Washington, DC: AASHTO.

15. ASTM International. 2018. *Standard Test Method for Slump Flow of Self-Consolidating Concrete*. ASTM C1611/C1611M-18. West Conshohocken, PA: ASTM International. https://doi.org/10.1520/C1611_C1611M-18.

16. Allena, S., and C. M Newtson. 2010. "Ultra-High Strength Concrete Mixtures Using Local Materials." Presented at the Concrete Sustainability Conference, Tempe, AZ. https://doi.org/10.13140/2.1.2465.3764.

17. Trejo-Arroyo, D. L., K. E. Acosta, J. C. Cruz, A. M. Valenzuela-Muñiz, R. E. Vega-Azamar, and L. F. Jiménez. 2019. "Influence of ZrO_2 Nanoparticles on the Microstructural Development of Cement Mortars with Limestone Aggregates." *Applied Sciences* 9 (3): 598. https://doi.org/10.3390/app9030598.

18. Han, B., Z. Wang, S. Zeng, D. Zhou, X. Yu, X. Cui, and J. Ou. 2017. "Properties and Modification Mechanisms of Nano-Zirconia Filled Reactive Powder." *Concrete Construction and Building Materials* 141: 426-434. https://doi.org/10.1016/j.conbuildmat.2017.03.036.

19. Schoepfer, J., and A. Maji. 2009 "An Investigation into the Effect of Silicon Dioxide Particle Size on the Strength of Concrete." *ACI Symposium Publication* 267: 45–58.

20. Graybeal, B. A. 2007. "Compressive Behavior of Ultra-High-Performance Fiber-Reinforced Concrete." *ACI Materials Journal* 104 (2): 146-152. https://doi.org/10.14359/18577.

21. ASTM International. 2018. *Standard Test Method for Flexural Strength of Concrete (Using Simple Beam with Third-Point Loading)*. ASTM C78/C78M-18. West Conshohocken, PA: ASTM International. https://doi.org/10.1520/C0078_C0078M-18.

22. Bayasi, Z., and J. Zhou. "Properties of Silica Fume Concrete and Mortar." 1993. *ACI Materials Journal* 90 (4): 349–356.

23. ASTM International. 2017. *Standard Test Method for Length Change of Hardened Hydraulic-Cement Mortar and Concrete*. ASTM C157/C157M-17. West Conshohocken, PA: ASTM International. https://doi.org/10.1520/C0157_C0157M-17.

24. Tadros, M. K., N. AL-Omaishi, S. J. Seguirant, and J. G. Gallt. 2003. *Prestress Losses in Pretensioned High-Strength Concrete Bridge Girders*. NCHRP (National Cooperative Highway Research Program) report 496. Washington, DC: NCHRP. https://onlinepubs.trb.org/onlinepubs/nchrp/nchrp_rpt_496.pdf.

25. ASTM International. 2015. *Standard Test Method for Creep of Concrete in Compression*. ASTM C512/C512M-15. West Conshohocken, PA: ASTM International. https://doi.org/10.1520/C0512_C0512M-15.

26. Taylor, C. W., B. D. Weldon, D. V. Jáuregui, and C. M. Newtson. 2013. "Case Studies Using Ultrahigh-Performance Concrete for Prestressed Girder Bridge Design." *Practice Periodical on Structural Design and Construction* 18 (4): 261–267. https://doi.org/10.1061/(ASCE)SC.1943-5576.0000167.

27. PCI. 2014. *Bridge Design Manual*. 3rd ed. MNL-133-14. Chicago, IL: PCI. https://doi.org/10.15554/MNL-133-14.

Notation

A_{Tf} = transformed area of girder section at time of service

A_{Ti} = transformed area of girder section at transfer

e_{tf} = distance between centers of gravity of strands and concrete section at time of service

e_{ti} = distance between centers of gravity of strands and concrete section at time of transfer

E_c = modulus of elasticity of concrete at erection

$f_{b,service}$ = concrete stress at bottom of girder at transfer length at time of service

$f_{b,transfer}$ = concrete stress at bottom of girder at transfer length at time of transfer

f'_c = design concrete compressive strength at final service conditions

f'_{ci} = design concrete compressive strength at time of transfer of the prestressing force

$f_{t,service}$ = concrete stress at top of girder at transfer length at time of service

$f_{t,transfer}$ = concrete stress at top of girder at transfer length at time of transfer

H = relative humidity

k_{hc} = humidity factor for creep

k_{hs} = shrinkage correction factor for ambient humidity

k_s = factor for the effect of the volume–to–surface area ratio of the component

k_{td} = time development factor

K_1 = correction factor for source of aggregates

K_2 = calibration factor for modulus of elasticity

M_{DC1} = unfactored moment due to girder self-weight

M_{DC2} = unfactored moment due to slab and haunch weight

M_{DC3} = unfactored moment due to barrier weight

M_{DW} = unfactored moment due to future wearing surface

$M_{g,transfer}$ = moment at transfer length section due to girder weight, based on total girder length

$M_{(LL+IM)HL93}$ = maximum service live load moment at midspan (including truck and lane loading)

M_n = flexural capacity

P_f = effective force in prestressing strands after all losses

P_{pi} = initial prestressing force immediately before transfer

S_{bf} = section modulus for the bottom extreme fiber of the composite section at service stage

S_{bfC} = section modulus for the bottom extreme fiber of the composite section

S_{bi} = section modulus for bottom extreme fiber of the girder section at transfer

S_{tf} = section modulus for the top extreme fiber of the composite section at service stage

S_{tfC} = section modulus for the top extreme fiber of the composite section

S_{ti} = section modulus for the top extreme fiber of the girder section at transfer

t = age of concrete between the end of curing and the time to consider shrinkage effect

V/S = volume-to-surface area ratio

w_c = unit weight (density) of concrete

w/b = water-binder ratio

ε_{sh} = shrinkage strain

ϕ = resistance factor

Appendix A: Chemical composition of silica fume and fly ash

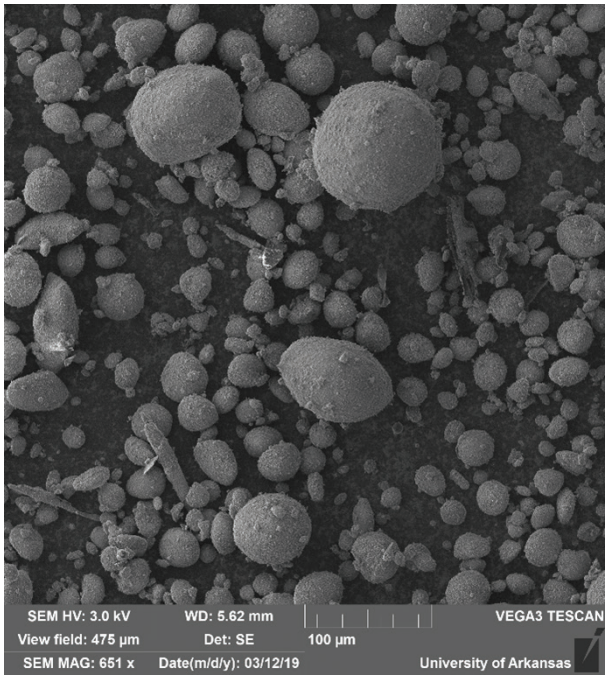

Densified gray silica fume

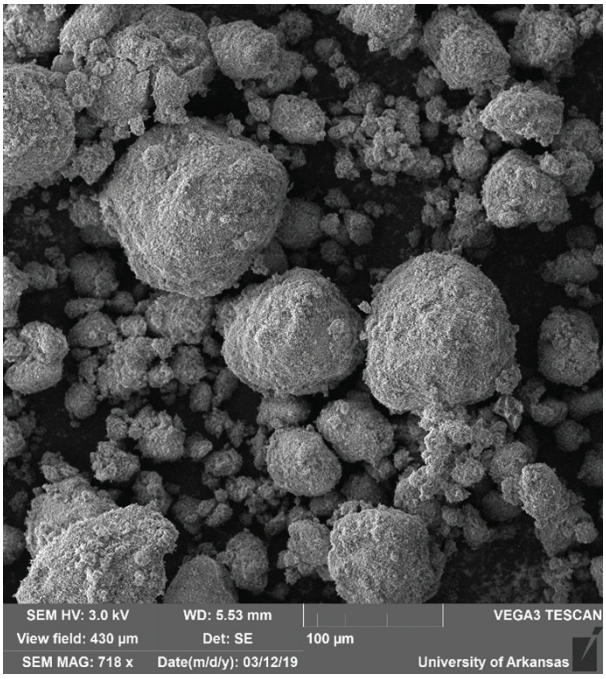

Undensified white silica fume

Figure A.1. Scanning electron microscopy imaging of densified gray silica fume and undensified white silica fume.

Table A.1. X-ray fluorescence analysis of the oxide content percentage in the two types of silica fume and in the fly ash used in the study

Oxide	Undensified white silica fume, %	Densified gray silica fume, %	Fly ash, %
SiO_2	92.37	86.18	31.68
Al_2O_3	0.41	0.35	17.62
Fe_2O_3	0.36	1.27	4.34
CaO	0.07	0.45	18.50
MgO	0.06	2.21	5.00
SO_3	0.16	0.33	1.58
Na_2O	0.08	0.2	2.22
K_2O	0.04	0.75	0.4
TiO_2	0.03	0.01	1.02
P_2O_5	0.31	0.07	0.99
Mn_2O_3	ND	0.16	0.02
SrO	ND	0.01	0.24
Cr_2O_3	0.01	0.02	0.02
PbO	0.03	0.02	0.01
CuO	0.07	002	0.02
ZnO	ND	0.08	0.02
BaO	ND	ND	0.13
ZrO_2	4.61	ND	0.02
Cl^-	0.04	0.09	0.01
F^-	ND	ND	0.33
LOI	1.15	7.77	15.77

Note: LOI = loss on ignition; ND = not detected.

Appendix B: Girder design example

Material properties used in bridge design

Modulus of elasticity of prestressing strands E_s = 29,000 ksi

Concrete unit weight w_c = 150.0 lb/ft^3

Compressive strength of deck concrete f'_c = 10.0 ksi

Bridge geometry

Total bridge width: 75.0 ft

Girder spacing: 8.5 ft

Number of girders: 9

Parapet width: 1.5 ft

Deck thickness: 7.0 in.

Haunch thickness: 2.0 in.

Notation

A = cross-sectional area

e = distance between centers of gravity of strands and concrete section

E_s = modulus of elasticity of reinforcing steel

f'_c = design concrete compressive strength at final service conditions

I = moment of inertia

S_{bottom} = section modulus from the extreme bottom fiber of girder

S_{top} = section modulus from the extreme top of the girder

Y_{bottom} = distance from neutral axis to extreme bottom fiber of precast concrete girder

Y_{top} = distance from neutral axis to extreme top fiber of precast concrete girder or composite section

w_c = concrete unit weight

Table B.1. Modulus of elasticity of ultra-high-strength concrete used in the girder design

MOE	UHSC-17	UHSC-20	UHPC-24	Bridge deck
Initial MOE, ksi	6774.39	7291.95	6324.56	n/a
Final MOE, ksi	6877.20	8217.66	7745.97	6062.49

Note: MOE = modulus of elasticity; n/a = not applicable; UHPC-24 = 24 ksi compressive strength ultra-high-performance concrete; UHSC-17 = 17 ksi compressive strength ultra-high-strength concrete; UHSC-20 = 20 ksi compressive strength ultra-high-strength concrete. 1 ksi = 6.895 MPa.

Table B.2. Concrete section properties for UHSC-17 girder

Property	Gross section properties	Transformed section properties		
		At 1 day	At 90 days	Composite girder and deck
A, in.^{2}	1503.50	1581.20	1579.70	2259.60
I, in.^{4}	2,964,530.45	3,130,831.45	3,127,737.27	5,669,247.53
Y_{bottom}, in.	54.19	51.86	51.90	73.88
Y_{top}, in.	65.81	68.14	68.10	46.12
e, in.	47.44	42.94	42.98	67.13
S_{bottom}, in.^{3}	54,708.10	60,375.00	60,264.90	76,730.80
S_{top}, in.^{3}	45,045.50	45,944.70	45,928.50	122,937.00

Note: A = cross sectional area; e = distance between centers of gravity of strands and concrete section; I = moment of inertia; S_{bottom} = section modulus from the extreme bottom fiber of girder; S_{top} = section modulus from the extreme top of the girder; UHSC-17 = 17 ksi compressive strength ultra-high-strength concrete; Y_{bottom} = distance from neutral axis to extreme bottom fiber of precast concrete girder; Y_{top} = distance from neutral axis to extreme top fiber of precast concrete girder or composite section. 1 in. = 25.4 mm; 1 in.^{2} = 645.2 mm^2; 1 in.^{3} = 16,390 mm^3; 1 ksi = 6.895 MPa.

Table B.3. Concrete section properties for UHSC-20 girder

Property	Gross section properties	Transformed section properties		
		At 1 day	At 90 days	Composite girder and deck
A, in.^{2}	1503.50	1574.00	1563.37	2160.94
I, in.^{4}	2,964,530.45	3,116,089.00	3,094,103.21	5,375,908.98
Y_{bottom}, in.	54.19	52.06	52.37	72.45
Y_{top}, in.	65.81	67.94	67.63	47.55
e, in.	47.44	45.31	45.62	65.70
S_{bottom}, in.^{3}	54,708.10	59,852.10	59,080.00	74,205.41
S_{top}, in.^{3}	45,045.50	45,867.40	45,751.40	11,3049.27

Note: A = cross sectional area; e = distance between centers of gravity of strands and concrete section; I = moment of inertia; S_{bottom} = section modulus from the extreme bottom fiber of girder; S_{top} = section modulus from the extreme top of the girder; UHSC-20 = 20 ksi compressive strength ultra-high-strength concrete; Y_{bottom} = distance from neutral axis to extreme bottom fiber of precast concrete girder; Y_{top} = distance from neutral axis to extreme top fiber of precast concrete girder or composite section. 1 in. = 25.4 mm; 1 in.^{2} = 645.2 mm^2; 1 in.^{3} = 16,390 mm^3; 1 ksi = 6.895 MPa.

Table B.4. Concrete section properties for UHPC-24 girder

Property	Gross section properties	Transformed section properties		
		At 2 days	At 90 days	Composite girder and deck
A, in.^{2}	1503.50	1588.40	1568.47	2202.40
I, in.^{4}	2,964,530.45	3,145,470.40	3,104,686.43	5,497,383.00
Y_{bottom}, in.	54.19	51.65	52.22	73.16
Y_{top}, in.	65.81	68.35	67.78	46.84
e, in.	47.44	44.90	45.47	66.41
S_{bottom}, in.^{3}	54,708.10	60,898.30	59,450.50	75,140.00
S_{top}, in.^{3}	45,045.50	46,020.87	45,807.40	11,7369.90

Note: A = cross sectional area; e = distance between centers of gravity of strands and concrete section; I = moment of inertia; S_{bottom} = section modulus from the extreme bottom fiber of girder; S_{top} = section modulus from the extreme top of the girder; UHPC-24 = 24 ksi compressive strength ultra-high-performance concrete; Y_{bottom} = distance from neutral axis to extreme bottom fiber of precast concrete girder; Y_{top} = distance from neutral axis to extreme top fiber of precast concrete girder or composite section. 1 in. = 25.4 mm; 1 in.^{2} = 645.2 mm^2; 1 in.^{3} = 16,390 mm^3; 1 ksi = 6.895 MPa.

Table B.5. Dead and live load moments used in the flexural design of the girders

Moment type	Magnitude, kip-ft/girder
Moment due to girder self-weight	17,152.43
Moment due to slab, stay-in-place forms, and haunch weight	9287.30
Moment due to barrier weight	1149.38
Moment due to future wearing surface	3258.22
Maximum service live load moment at midspan (including truck and lane loading)	9713.10

Note: 1 kip-ft = 1.356 kN-m.

About the authors

Ahmed Al Mohammedi, PhD, is a researcher in the Department of Science and Technology at the Ministry of Higher Education and Scientific Research of Iraq. He received his PhD in civil engineering from the University of Arkansas in Fayetteville and was awarded PCI's Dennis R. Mertz Bridge Research Fellowship in 2018. His research interests include mixture proportioning and prestressed concrete.

Cameron D. Murray, PhD, PE, is an assistant professor in the Department of Civil Engineering at the University of Arkansas. He received his bachelor's and master's degrees in civil engineering from the University of Arkansas and his PhD from the University of Oklahoma in Norman. His research interests include prestressed concrete, alkali-silica reaction, and rapid-setting concrete.

Canh N. Dang, PhD, PE, is a structural engineer at Thornton Tomasetti in Ho Chi Minh City, Vietnam. He received his bachelor's and master's degrees from the Ho Chi Minh City University of Technology and his PhD from the University of Arkansas. His research interests include concrete materials, mixture proportioning, and prestressed concrete.

W. Micah Hale, PhD, PE, is a professor in the Department of Civil Engineering at the University of Arkansas. He received his bachelor's and master's degrees and PhD from the University of Oklahoma and is a licensed professional engineer in Arkansas. His research interests include concrete materials, mixture proportioning, and prestressed concrete.

Abstract

This paper focuses on developing ultra-high-strength concrete (UHSC) with mechanical properties comparable to those of ultra-high-performance concrete (UHPC) and with production procedures similar to those used for high-strength concrete. A concrete mixture was developed to achieve a compressive strength of 17 ksi (117 MPa) at 28 days without using silica fume and with a slump flow as high as 35 in. (889 mm). Another concrete mixture with compressive strength of 20 ksi (138 MPa) was designed using only 130 lb/yd^3 (77.1 kg/m^3) of silica fume. In addition to these two mixtures, a UHPC mixture was also designed with a compressive strength of 24 ksi (165 MPa). Laboratory tests were conducted to investigate predictions of modulus of elasticity, flexural strength, creep, and shrinkage for the developed mixtures. This paper demonstrates that using UHSC and 0.7 in. (18 mm) diameter strands will produce adequate flexural strength to design 300 ft (91.4 m) long prestressed concrete I-girders that have service stresses within safe limits.

Keywords

Bridge girder, creep, modulus of elasticity, modulus of rupture, shrinkage, UHPC, UHSC, ultra-high-performance concrete, ultra-high-strength concrete.

Review policy

This paper was reviewed in accordance with the Precast/Prestressed Concrete Institute's peer-review process. The Precast/Prestressed Concrete Institute is not responsible for statements made by authors of papers in *PCI Journal*. No payment is offered.

Publishing details

This paper appears in *PCI Journal* (ISSN 0887-9672) V. 67, No. 3, May–June 2022, and can be found at https://doi.org/10.15554/pcij67.3-01. *PCI Journal* is published bimonthly by the Precast/Prestressed Concrete Institute, 8770 W. Bryn Mawr Ave., Suite 1150, Chicago, IL 60631.

Reader comments

Please address any reader comments to *PCI Journal* editor-in-chief Tom Klemens at tklemens@pci.org or Precast/Prestressed Concrete Institute, c/o *PCI Journal*, 8770 W. Bryn Mawr Ave., Suite 1150, Chicago, IL 60631.